Int. J. Heat Mass Transfer. Vol. 32, No. 8, pp. 1431–1442, 1989
Printed in Great Britain

0017–9310/89 $3.00 + 0.00

Mixed convection along slender vertical cylinders with variable surface temperature

J. J. HECKEL,† T. S. CHEN and B. F. ARMALY
Department of Mechanical and Aerospace Engineering, University of Missouri–Rolla, Rolla, MO 65401, U.S.A.

(*Received* 27 *May* 1988 *and in final form* 22 *November* 1988)

Abstract—Mixed convection in laminar boundary layer flow along slender vertical cylinders is analyzed for the situation in which the surface temperature $T_w(x)$ varies arbitrarily with the axial coordinate x. It covers the entire mixed convection regime from pure free convection ($\chi = 0$) to pure forced convection ($\chi = 1$), where $\chi = [1 + (Gr_x/Re_x^2)^{1/4}]^{-1}$ is the mixed convection parameter. The governing boundary layer equations along with the boundary conditions are first cast into a dimensionless form by a non-similar transformation and the resulting system of equations is then solved by a weighted finite-difference method of solution in conjunction with cubic spline interpolation. Sample calculations are performed for the case of power law variation in surface temperature, $T_w(x) - T_\infty = ax^n$, for fluids with Prandtl numbers of 0.1, 0.7, 7, and 100 over a wide range of surface curvature parameters $0 \leqslant \Lambda \leqslant 50$ (or $0 \leqslant \xi \leqslant 5$). Local and average Nusselt numbers are presented. It is found that the local Nusselt number in the form $Nu_x/(Re_x^{1/2} + Gr_x^{1/4})$ increases with increasing surface curvature, Prandtl number, and the exponent n, but for low values of Λ, it initially decreases and then increases as χ goes from 0 to 1. As curvature increases a linear relationship is found to exist between the Nusselt number and the mixed convection parameter. Correlation equations for the local and average Nusselt numbers are also presented.

INTRODUCTION

THERE have been relatively few studies on mixed convection along a vertical cylinder. Chen and Mucoglu [1, 2] were the first to analyze the effects of buoyancy forces on forced convection along vertical cylinders for the case of uniform wall temperature (UWT) and uniform surface heat flux (UHF). They used the local non-similarity method of solution to obtain heat transfer results that cover the surface curvature parameter, $\Lambda_F = 2(x/r_0)\, Re_x^{-1/2}$, from 0 to 8 for Prandtl numbers of 0.7 and 7. Bui and Cebeci [3] analyzed the UWT case for $Pr = 0.1$, 1.0, and 10 for curvatures up to $\Lambda_F = 10$ using a central difference finite-difference method of solution. Reference [1] and the study by Bui and Cebeci for the UWT case use a mixed convection parameter $\Omega_x = Gr_x/Re_x^2$ which varies from zero for pure forced convection to infinity for pure free convection. Reference [2] presents the UHF case with a mixed convection parameter $\Omega_x^* = Gr_x^*/Re_x^{5.2}$. Recently, Lee *et al.* [4] analyzed the UWT case for slender vertical cylinders using a new mixed convection parameter $\chi = (1 + \Omega_x^{1/4})^{-1}$ which varies from zero for pure free convection to one for pure forced convection. They also treated the UHF case [5] using the mixed convection parameter $\chi^* = (1 + \Omega_x^{*1/5})^{-1}$, which also varies from zero for pure free convection to one for pure forced convection. The main difficulty encountered in these studies has been the numerical solutions for large surface curvatures. The results of refs. [1, 2] agree well with those of Lee *et al.* [4, 5] up to surface curvatures $\Lambda = 2(x/r_0)(Re_x^{1/2} + Gr_x^{1/4})^{-1}$ for UWT or $\Lambda^* = 2(x/r_0)(Re_x^{1/2} + Gr_x^{*1/5})^{-1}$ for UHF of 8 for $Pr = 0.7$ and 7.0. However, the results of Bui and Cebeci are about 36% higher for large surface curvatures. Lee *et al.* [4] attributed this to the latter's use of a central difference finite-difference method of solution which has difficulty handling the boundary layer equations as they become 'stiff' with increasing curvature. Lee *et al.* [4, 5] advocate the use of a weighted difference finite-difference method [6] along with a cubic spline interpolation scheme [7] to overcome the difficulties associated with high values of curvature or Prandtl number. Another advantage of the analysis by Lee *et al.* [4, 5] is that it was applied to the full range of mixed convection, from pure free convection to pure forced convection.

The problem of natural convection along a vertical cylinder has been extensively studied [8–14]. Elenbaas [8] used Langmuir's stagnant film model to evaluate the heat transfer coefficients for vertical cylinders under the UWT condition. Sparrow and Gregg [9] reworked this same problem using a power series solution for $Pr = 0.72$ and 1 covering surface curvatures $\Lambda_N = 2(x/r_0)\, Gr_x^{-1/4}$ of up to about 1.5. Kuiken [10] also applied the power series expansion method to investigate some non-uniform wall temperature conditions and obtained results for $0.7 \leqslant Pr \leqslant 10$. Similarly, Fujii and Uehara [11] treated the case of variable wall temperature and obtained results, again by the

†Present address: Department of Mechanical Engineering, U.S. Military Academy, West Point, NY 10996, U.S.A.

NOMENCLATURE

C_{f_x} local skin friction coefficient, $2\tau_w/\rho u_\infty^2$

$\overline{C_{f_L}}$ average skin friction coefficient, $(2/\rho u_\infty^2 L)\int_0^L \tau_w\,dx$

f reduced stream function, $(\psi/\nu r_0)(Re_x^{1/2}+Gr_x^{1/4})^{-1}$

Gr_L, Gr_0 Grashof numbers, defined, respectively, as $g\beta[T_w(L)-T_\infty]L^3/\nu^2$ and $g\beta[T_w(r_0)-T_\infty]r_0^3/\nu^2$

Gr_x local Grashof number, $g\beta[T_w(x)-T_\infty]x^3/\nu^2$

Gr_x^* modified local Grashof number, $g\beta q_w(x)x^4/k\nu^2$

h local heat transfer coefficient, $q_w/(T_w-T_\infty)$

$\bar{h}$ average heat transfer coefficient

k thermal conductivity of the fluid

L arbitrary length of cylinder

m exponent used in the mixed convection correlation

n exponent in the power law variation of the surface temperature

$\overline{Nu}_L$ average Nusselt number, $\bar{h}L/k$

Nu_x local Nusselt number, hx/k

Pr Prandtl number, ν/α

r radial coordinate

r_0 radius of the cylinder

Re_L, Re_0 Reynolds number based on L and r_0, respectively, as $u_\infty L/\nu$ and $u_\infty r_0/\nu$

Re_x Reynolds number based on x, $u_\infty x/\nu$

T fluid temperature

u axial velocity component

v radial velocity component

x axial coordinate

y transverse coordinate

z dimensionless axial coordinate, x/r_0.

θ dimensionless temperature, $(T-T_\infty)/[T_w(x)-T_\infty]$

Λ curvature parameter for mixed convection with variable surface temperature, $(2x/r_0)(Re_x^{1/2}+Gr_x^{1/4})^{-1}$

Λ^* curvature parameter for mixed convection with variable surface heat flux, $(2x/r_0)(Re_x^{1/2}+Gr_x^{*1/5})^{-1}$

Λ_F curvature parameter for pure forced convection, $(2x/r_0)Re_x^{-1/2}$

Λ_N curvature parameter for natural convection with variable surface temperature, $(2x/r_0)Gr_x^{-1/4}$

Λ_N^* modified curvature parameter for natural convection with variable surface heat flux, $(2x/r_0)\,Gr_x^{*-1/5}$

ν kinematic viscosity

ξ dimensionless axial coordinate $[x/(r_0 Re_0)]^{1/4}$ or $[\Lambda/(2\chi)]^{1/2}$

τ_w local wall shear stress

ψ stream function

χ mixed convection parameter for variable surface temperature, $(1+\Omega_x^{1/4})^{-1}$

χ^* mixed convection parameter for variable surface heat flux, $(1+\Omega_x^{*1/5})^{-1}$

Ω_x buoyancy parameter for variable surface temperature, Gr_x/Re_x^2

Ω_x^* buoyancy parameter for variable surface heat flux, $Gr_x^*/Re_x^{5/2}$

Ω_0 modified buoyancy parameter, $[Gr_0/Re_0^{1-n}]^{1/4}$.

Greek symbols

α thermal diffusivity

β volumetric coefficient of thermal expansion

η pseudo-similarity variable, $[(r^2-r_0^2)/2r_0x](Re_x^{1/2}+Gr_x^{1/4})$

Subscripts

F pure forced convection

N pure natural convection

p flat plate

w conditions at the wall

∞ conditions at the free stream.

power series solution, for $0.72 \leqslant Pr \leqslant 100$ covering Λ_N from 0 to 2.73. To overcome truncation errors of the power series and the local similarity solution, Minkowycz and Sparrow [12] employed the local nonsimilarity method of solution and obtained results for $Pr = 0.733$ covering $0 \leqslant \Lambda_N \leqslant 10$. Kuiken [13] presented a power series solution for the UWT condition that can be applied to the thick boundary layer along vertical slender cylinders. Lee *et al.* [4, 5] examined both the UWT and UHF cases of natural convection along a vertical cylinder as part of their mixed convection study and employed a weighted finite-difference method designed to overcome the difficulties associated with increasing curvature. As a result, they were able to obtain results up to $\Lambda_N = 50$ for $0.1 \leqslant Pr \leqslant 100$. The findings of Lee *et al.* [4] demonstrated that the central difference scheme used by Bui and Cebeci [3] produces large errors as the cur-

vature increases. Recently, Lee *et al.* [14] treated the variable wall temperature problem for natural convection along slender vertical cylinders and presented results for power law variation in the wall temperature. They found that the results of ref. [4] are inaccurate for $\Lambda_N > 10$ due to the use of an improper step size $\Delta\eta$ and that those of Fujii and Uehara [11] are valid only for Λ_N up to about 1.5. Similar inaccuracies in the results of ref. [5] were found for $\Lambda_N^* > 10$ by the present authors in a study of natural convection along slender vertical cylinders with variable surface heat flux [15]. In that study [15] results were presented for the case of power law variation in the surface heat flux, $q_w(x) = ax^n$, with $-0.5 \leqslant n \leqslant 0.5$, for $0.1 \leqslant Pr \leqslant 100$, and $0 \leqslant \Lambda_N^* \leqslant 50$.

For comparison purposes, results for mixed convection along a vertical flat plate are needed. There are numerous studies on mixed convection along a vertical flat plate (see, e.g. refs. [16–21]). The Nusselt number results for this flow geometry have been correlated by Churchill [22] using the simple form $Nu^m = Nu_F^m + Nu_N^m$, with $m = 3$, where Nu_F is the Nusselt number for pure forced convection and Nu_N is the Nusselt number for pure free convection. Extensive correlations for mixed convection along vertical, inclined, and horizontal flat plates have been carried out [16] and verified with experimental data for air [17].

From the past studies, it is clear that the results for mixed convection under the UWT condition at high values of curvature need to be reassessed. In addition, the combined effects of variable surface temperature and curvature on the flow and heat transfer in mixed convection along slender vertical cylinders have not been studied for the entire mixed convection regime. This has motivated the present study.

ANALYSIS

Consider a semi-infinite, vertical cylinder with radius r_0 that is aligned parallel to a uniform, laminar free stream with velocity u_∞ and temperature T_∞. The axial coordinate x is measured in the direction of the forced flow and the radial coordinate r is measured from the axis of the cylinder. The surface of the cylinder is subjected to an arbitrary variation in temperature $T_w(x)$, and the gravitational acceleration g is acting downward. Fluid properties are assumed to be constant except for variations in density which induce the buoyancy force. By employing the laminar boundary layer assumptions and making use of the Boussinesq approximation, the governing conservation equations can be written as

$$\frac{\partial}{\partial x}(ru) + \frac{\partial}{\partial r}(rv) = 0 \tag{1}$$

$$u\frac{\partial u}{\partial x} + v\frac{\partial u}{\partial r} = \frac{\nu}{r}\frac{\partial}{\partial r}\left(r\frac{\partial u}{\partial r}\right) \pm g\beta(T - T_\infty) \tag{2}$$

$$u\frac{\partial T}{\partial x} + v\frac{\partial T}{\partial r} = \frac{\alpha}{r}\frac{\partial}{\partial r}\left(r\frac{\partial T}{\partial r}\right). \tag{3}$$

The positive sign in equation (2) applies to upward forced flow and the negative sign to downward forced flow. In these equations, u and v are the velocity components in the x- and r-directions, respectively; T is the fluid temperature; and ν, β, and α are, respectively, the kinematic viscosity, the volumetric coefficient of thermal expansion, and the thermal diffusivity of the fluid.

The boundary conditions are

$$u = v = 0, \quad T = T_w(x) \quad \text{at } r = r_0 \tag{4}$$

$$u \to u_\infty, \quad T \to T_\infty \quad \text{as } r \to \infty \tag{5}$$

$$u = u_\infty, \quad T = T_\infty \quad \text{at } x = 0, r \geqslant r_0. \tag{6}$$

In writing equation (6) it is assumed that the flow and thermal boundary layer thicknesses are zero at the leading edge of the cylinder surface.

The conservation equations and the boundary conditions are then transformed into a dimensionless form by introducing the following dimensionless variables:

$$\eta = \frac{(r^2 - r_0^2)}{2r_0 x}(Re_x^{1/2} + Gr_x^{1/4}), \quad z = \frac{x}{r_0} \tag{7}$$

$$f(z,\eta) = \psi(x,r)/[\nu r_0(Re_x^{1/2} + Gr_x^{1/4})],$$

$$\theta(z,\eta) = (T - T_\infty)/[T_w(x) - T_\infty] \tag{8}$$

$$\Omega_x = \frac{Gr_x}{Re_x^2}, \quad \chi = (1 + \Omega_x^{1/4})^{-1} \tag{9}$$

where $Gr_x = g\beta[T_w(x) - T_\infty]x^3/\nu^2$ is the local Grashof number, $Re_x = u_\infty x/\nu$ the local Reynolds number, η the pseudo-similarity variable, z the dimensionless axial coordinate, $f(z,\eta)$ the reduced stream function, $\theta(z,\eta)$ the dimensionless temperature, $\psi(x,r)$ the stream function that satisfies the continuity equation, with $u = (\partial\psi/\partial r)/r$ and $v = -(\partial\psi/\partial x)/r$, Ω_x the buoyancy parameter which varies from zero for pure forced convection to infinity for pure free convection, and χ is the mixed convection parameter which varies from zero for pure free convection to one for pure forced convection.

The transformation yields

$$(1+\eta\Lambda)f''' + \Lambda f'' + \tfrac{1}{4}[2 + (1-\chi)(\gamma+1)]ff'' - \tfrac{1}{2}(1-\chi)(\gamma+1)f'^2 \pm (1-\chi)^4\theta = -z\left(f''\frac{\partial f}{\partial z} - f'\frac{\partial f'}{\partial z}\right) \tag{10}$$

$$(1+\eta\Lambda)\theta'' + \Lambda\theta' + \frac{Pr}{4}[2 + (1-\chi)(\gamma+1)]f\theta' - Pr\,\gamma f'\theta = -Pr\,z\left(\theta'\frac{\partial f}{\partial z} - f'\frac{\partial\theta}{\partial z}\right) \tag{11}$$

$$f(z,0) = f'(z,0) = 0, \quad \theta(z,0) = 1$$
$$f'(z,\infty) = \chi^2, \quad \theta(z,\infty) = 0 \tag{12}$$

where

$$\Lambda = 2\frac{x}{r_0}(Re_x^{1/2} + Gr_x^{1/4})^{-1} \tag{13}$$

is the mixed convection curvature parameter and

$$\gamma = \frac{x}{T_w(x) - T_\infty}\frac{\mathrm{d}}{\mathrm{d}x}[T_w(x) - T_\infty]. \tag{14}$$

The primes in equations (10)–(12) denote partial differentiation with respect to η, and the plus and minus signs in front of the term $(1-\chi)^4\theta$ in equation (10) now represent buoyancy assisting flow and buoyancy opposing flow, respectively.

The system of equations (10)–(12) represents the general form of the transformed boundary layer equations for variable wall temperature $T_w(x)$ along vertical cylinders in mixed convection. For the case of power law wall temperature distribution, $T_w(x) = T_\infty + ax^n$, one has from equation (14) that

$$\gamma = n. \tag{15}$$

Equations (10)–(12) contain three x-dependent parameters, $z(x)$, $\Lambda(x)$, and $\chi(x)$. These parameters can be related to a single x-dependent parameter $\xi(x)$ defined by

$$\xi = \left(\frac{z}{Re_0}\right)^{1/4}. \tag{16}$$

Thus

$$z(x) = Re_0\,\xi^4, \quad \Lambda = 2\xi^2\chi, \quad \chi = (1+\Omega_0\xi^{1+n})^{-1} \tag{17}$$

where

$$\Omega_0 = [Gr_0/Re_0^{1-n}]^{1/4} \tag{18}$$

with $Gr_0 = Gr_x$ and $Re_0 = Re_x$ for $x = r_0$. Also, the right-hand sides of equations (10) and (11) become, respectively

$$-\frac{1}{4}\xi\left(f''\frac{\partial f}{\partial \xi} - f'\frac{\partial f'}{\partial \xi}\right), \quad -\frac{Pr}{4}\xi\left(\theta'\frac{\partial f}{\partial \xi} - f'\frac{\partial \theta}{\partial \xi}\right). \tag{19}$$

Equations (10)–(12) can be rewritten as, with $\gamma = n$

$$(1+a_1\eta)f''' + a_1 f'' + a_2 ff'' + a_3 f'^2 + a_4\theta = a_5\left(f''\frac{\partial f}{\partial \xi} - f'\frac{\partial f'}{\partial \xi}\right) \tag{20}$$

$$(1+a_1\eta)\theta'' + a_1\theta' + Pr\,a_2 f\theta' + Pr\,a_6 f'\theta = Pr\,a_5\left(\theta'\frac{\partial f}{\partial \xi} - f'\frac{\partial \theta}{\partial \xi}\right) \tag{21}$$

$$f(\xi,0) = f'(\xi,0) = 0, \quad \theta(\xi,0) = 1$$
$$f'(\xi,\infty) = \chi^2, \quad \theta(\xi,\infty) = 0 \tag{22}$$

where

$$a_1 = \Lambda, \quad a_2 = \tfrac{1}{4}[2+(1-\chi)(n+1)]$$
$$a_3 = \tfrac{1}{2}(\chi-1)(n+1), \quad a_4 = \pm(1-\chi)^4$$
$$a_5 = -\xi/4, \quad a_6 = -n. \tag{23}$$

With Λ and χ related to ξ and Ω_0, the functions f and θ in equations (20)–(22) are functions of (ξ,η) and depend on three constant parameters n, Pr, and Ω_0. These equations are now in the form that can be solved by the method proposed by Lee *et al.* [6]. For the purpose of comparisons, the problem of mixed convection along a vertical flat plate with a power law variation in the wall temperature was also solved. The governing equations and boundary conditions have exactly the same form as equations (20)–(23) with the exceptions that for this case

$$\eta = \frac{y}{x}(Re_x^{1/2} + Gr_x^{1/4})$$

$$\xi = \chi, \quad \Lambda = 0, \quad a_5 = (1+n)(1-\chi)x/4. \tag{24}$$

It should be noted that this problem must be solved numerically from $\chi = 1$ to 0.

The physical quantities of interest include the local and average Nusselt numbers, the local and average friction factors, the axial velocity distribution, and the temperature profile. The local Nusselt number and the local friction factor can be expressed as

$$Nu_x/(Re_x^{1/2} + Gr_x^{1/4}) = -\theta'(\xi,0) \tag{25}$$
$$C_{f_x}Re_x^{1/2} = 2\chi^{-3}f''(\xi,0). \tag{26}$$

The average Nusselt number and the average friction factor can be expressed as

$$\overline{Nu}_L/(Re_L^{1/2} + Gr_L^{1/4}) = -4\chi_L\xi_L^{-2}\int_0^{\xi_L}\frac{\theta'(\xi,0)}{\chi}\xi\,\mathrm{d}\xi \tag{27}$$

$$\overline{C_{f_L}}Re_L^{1/2} = 8\xi_L^{-2}\int_0^{\xi_L}\chi^{-3}f''(\xi,0)\xi\,\mathrm{d}\xi \tag{28}$$

where $\xi_L = \xi$ at $x = L$, and $\chi_L = \chi$ at $x = L$. The axial velocity distribution can be written as

$$\frac{u}{u_\infty} = \frac{f'(\xi,\eta)}{\chi^2} \tag{29}$$

and the temperature profile is given by $\theta(\xi,\eta) = (T-T_\infty)/(T_w-T_\infty)$.

METHOD OF SOLUTION

Equations (20)–(22) constitute a system of nonlinear partial differential equations in the (ξ,η) coordinates with parameters Pr, n, and Ω_0 when Λ and χ are properly related to ξ (see equation (17)). The method described in refs. [4, 6] was employed to solve this system of equations. The details of the solution procedure parallel those described in them and, to conserve space, they are omitted here. It suffices to

mention some of the highlights. The f and θ equations are first converted into quasi-linear differential equations which, along with the corresponding boundary conditions, are then cast into finite-difference equations with a proper use of weighting factors. This allows the numerical scheme to shift automatically from the central difference algorithm to the upwind algorithm, and vice versa. The resulting system of algebraic equations is then solved numerically by the Gaussian elimination method in conjunction with the cubic spline interpolation procedure [7]. For large values of Λ, equations (20) and (21) become 'stiff' (i.e. they behave as second-order and first-order equations, respectively, in the wall region where η is very small). To solve stiff equations numerically, an upwind scheme or an equivalent scheme is required.

To obtain accurate numerical results, a proper choice of the step size $\Delta\eta$ and the dimensionless boundary layer thickness, η_∞, is important. It was found that as ξ is increased, η_∞ needs to be increased. The value of η_∞ was initially set to 15 at $\xi = \Lambda = 0$ and was increased gradually by an increment of 5 to $\eta_\infty = 45$ for $\xi = 5$ or $\Lambda = 50$. A step size of $\Delta\eta = 0.01$ was used, even though $\Delta\eta = 0.02$ would have been adequate. The step size in the ξ-direction did not appreciably affect the converged results and $\Delta\xi = 0.1$ was used. The numerical solution is an iterative scheme and a solution was considered to be convergent when the calculated values of f, f', and θ between two successive iterations differed by less than 10^{-4} at all nodes (i.e. at all η values for a given ξ).

RESULTS AND DISCUSSION

Numerical results were obtained for the case of buoyancy assisting flow. They cover Prandtl numbers of 0.1, 0.7, 7, and 100; values of Ω_0 of 0, 0.02, 0.1, 0.5, 1, 2 as well as the pure free convection case ($\Omega_0 = \infty$) for a power law temperature distribution of the form $T_w - T_\infty = ax^n$, with the exponent n varying in the range from $-0.4 \leqslant n \leqslant 0.5$ for mixed convection and $-0.5 \leqslant n \leqslant 0.5$ for pure free convection. These ranges are within the physical limits of n as determined in a manner outlined in Gebhart [23]. For pure forced convection the limits are $-0.5 \leqslant n$ and for pure free convection the physical limits are $-0.6 \leqslant n < 1.0$. The case of $\Omega_0 = 0$ corresponds to pure forced convection and $\Omega_0 = \infty$ corresponds to either $u_\infty = 0$ (pure free convection) or $r_0 = \infty$ (the flat plate solution in mixed convection with $\Lambda = 0$).

First, the results for pure free convection will be presented. The results of Lee *et al.* [14] for the UWT case ($n = 0$) were recalculated using a smaller step size of $\Delta\eta^* = 0.01$ and a variable η^*_∞ which was allowed to increase to 45. The radial coordinate η^* used in ref. [14] is related to η by $\eta^* = \eta/\sqrt{2}$. As an example, for $Pr = 0.7$, the present calculations for $\Lambda_N = 50$ using $\Delta\eta^* = 0.035$ and $\eta^*_\infty = 7.071$, as used in ref. [4], yield the result $Nu_x Gr_x^{-1/4} = 16.1$, whereas calculations using $\Delta\eta^* = 0.0125$ and $\eta^*_\infty = 30$, as used in ref. [14], give $Nu_x Gr_x^{-1/4} = 6.93$. For $\Delta\eta^* = 0.01$ and $\eta^*_\infty = 45$, the present calculation gives $Nu_x Gr_x^{-1/4} = 6.46$ and further reductions in $\Delta\eta^*$ or increases in η^*_∞ did not appreciably change the local Nusselt number. This led to the choice of $\Delta\eta^* = 0.01$ and a variable η^*_∞ up to 45 in the numerical calculations.

The $Nu_x Gr_x^{-1/4}$ results for pure free convection are listed in Table 1. It demonstrates that the local Nusselt number increases with increasing curvature and increasing Prandtl number for all n values investigated. It also shows that as the curvature increases both the effects of Pr and n decrease and the local Nusselt numbers will converge to an asymptotic value. This is anticipated because as the curvature increases the first two terms in the energy equation become dominant and the equation becomes independent of both Pr and n.

Figure 1 shows the effect of surface curvature on the local Nusselt number for the UWT case ($n = 0$). It is seen that as the curvature parameter Λ_N increases from 0, the local Nusselt number ratio, $Nu_x/Nu_{x,p}$, where $Nu_{x,p}$ is the local Nusselt number for the flat plate, increases from 1 and that it increases at a faster relative rate for lower Prandtl numbers. Figure 2 illustrates the effect of the exponent n on the local Nusselt number for vertical flat plates ($\Lambda_N = 0$). It is seen that the local Nusselt number increases with increasing n. In addition, the Nusselt number ratio $Nu_x/Nu_{x,UWT}$ shows a slight dependence on the Prandtl number. The vertical flat plate problem has also been studied [24].

Next, the results for pure forced convection will be presented. Lee *et al.*'s results [4] for the UWT case were obtained using $\Delta\eta = 0.05$ and $\eta_\infty = 10$, which were found to be in error at high curvatures. As an example, for $Pr = 0.7$ and $n = 0$ the present calculations for $\Lambda_F = 50$ give $Nu_x Re_x^{-1/2} = 16.2$ using $\Delta\eta = 0.05$ and $\eta_\infty = 10$, which compares with $Nu_x Re_x^{-1/2} = 6.72$ using $\Delta\eta = 0.01$ and $\eta_\infty = 45$. Further decreases in $\Delta\eta$ and increases in η_∞ did not appreciably lower the value of $Nu_x Re_x^{-1/2}$, so the calculations were performed using $\Delta\eta = 0.01$ and η_∞ was varied up to 45.

The $Nu_x Re_x^{-1/2}$ results for pure forced convection are listed in Table 2. The table shows that as the curvature increases the local Nusselt number increases for all Pr and n that were investigated. As in the free convection case, it also shows that as the curvature increases, the effects of Pr and n diminish and the local Nusselt numbers will converge to an asymptotic value. Included in Table 2 are the $f''(\xi, 0)$ results. It should be noted that for pure forced convection the momentum equation is not coupled to the energy equation and thus $f''(\xi, 0)$ is independent of n and Pr. It is seen that as the curvature increases the value of $f''(\xi, 0)$ increases, as has been noted in other studies (for example, Seban and Bond [25]).

Figure 3 is a plot of $Nu_x/Nu_{x,p}$ vs Λ_F which shows that the local Nusselt number ratio increases from 1 as Λ_F increases from 0 and that it increases faster with

Table 1. The $Nu_x\,Gr_x^{-1/4}$ results for power law variation of surface temperature, free convection

	$Pr = 0.1$			$Pr = 0.7$			$Pr = 7$			$Pr = 100$		
	n			n			n			n		
ξ	−0.5	0	0.5	−0.5	0	0.5	−0.5	0	0.5	−0.5	0	0.5
0	0.0513	0.1638	0.2186	0.1093	0.3532	0.4598	0.2549	0.7455	0.9474	0.5494	1.5493	1.9522
0.5	0.1359	0.2616	0.3189	0.2040	0.4652	0.5659	0.3586	0.8541	1.0588	0.6554	1.6588	2.0642
1.0	0.3546	0.4946	0.5587	0.3867	0.7154	0.8351	0.6192	1.1376	1.3530	0.9413	1.9635	2.3786
1.5	0.7289	0.8522	0.9136	0.7674	1.0792	1.2144	0.9928	1.5516	1.7791	1.3585	2.4199	2.8536
2.0	1.2295	1.3238	1.3772	1.1688	1.5272	1.6813	1.4543	2.0646	2.2998	1.8697	2.9911	3.4517
2.5	1.8304	1.9017	1.9463	1.6780	2.0657	2.2310	1.9872	2.6642	2.9165	2.4521	3.6518	4.1470
3.0	2.5284	2.5822	2.6188	2.3316	2.7053	2.8706	2.5780	3.3369	3.6345	3.0900	4.3869	4.9245
3.5	3.3261	3.3666	3.3961	3.1353	3.4547	3.6095	3.2186	4.0860	4.4233	3.8597	5.1980	5.7828
4.0	4.2295	4.2594	4.2831	4.0762	4.3224	4.4598	3.9273	4.9187	5.2975	4.7248	6.2565	6.7352
4.5	5.2490	5.2714	5.2904	5.1394	5.3177	5.4353	4.7400	5.8295	6.2818	5.7093	7.2490	7.9254
5.0	6.4029	6.4200	6.4354	6.3251	6.4554	6.5547	5.7147	6.8771	7.3422	6.7810	8.5257	9.1301

increasing curvature for lower Prandtl numbers and becomes nearly linear at higher curvatures. This trend is similar to that for free convection. The effect of exponent n on the flat plate is illustrated in Fig. 4. As in free convection, the local Nusselt number increases with increasing n and the $Nu_x/Nu_{x,\mathrm{UWT}}$ ratio has a weak dependence on the Prandtl number.

Calculations for mixed convection were carried out using $\Delta\eta = 0.01$ and η_∞ was varied up to 45. The independent variable ξ was varied from 0 (corresponding to pure forced convection for the vertical flat plate, $\chi = 1$ and $\Lambda = 0$) to the point where either $\Lambda \geqslant 50$ or $\chi \leqslant 0.1$. The $Nu_x/(Re_x^{1/2} + Gr_x^{1/4})$ and $f''(\xi, 0)$ results were obtained for $Pr = 0.1$, 0.7, 7,

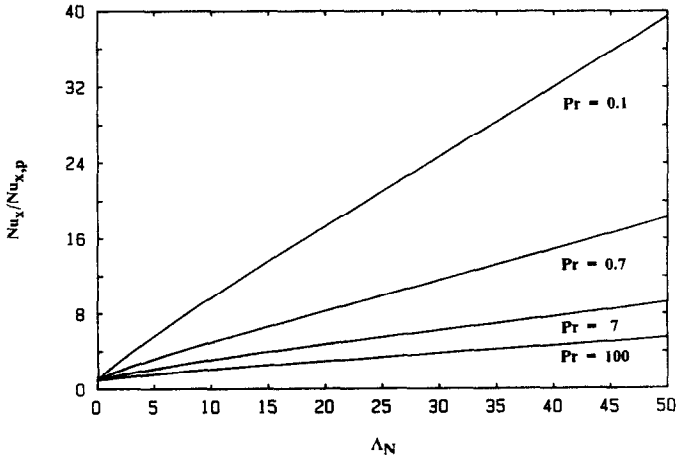

FIG. 1. $Nu_x/Nu_{x,\mathrm{p}}$ vs Λ_N for pure free convection, uniform wall temperature ($n = 0$).

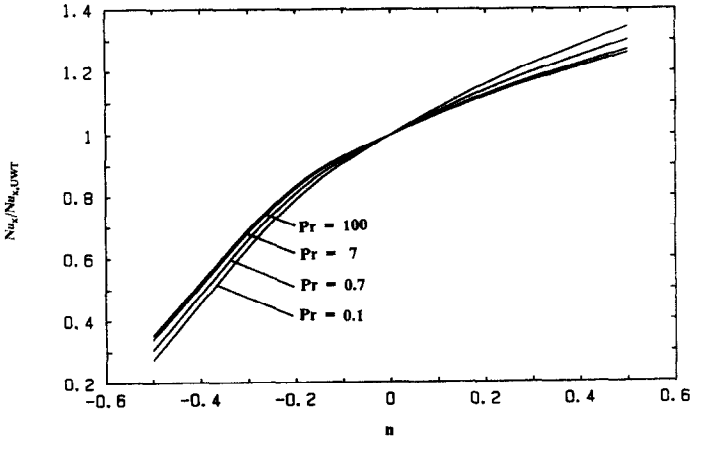

FIG. 2. $Nu_x/Nu_{x,\mathrm{UWT}}$ vs n for pure free convection, flat plates ($\Lambda_\mathrm{N} = 0$).

Table 2. The $Nu_x\,Re_x^{-1/2}$ and $f''(\xi,0)$ results for power law variation of surface temperature, forced convection

	$Pr = 0.1$			$Pr = 0.7$			$Pr = 7$			$Pr = 100$			
	n			n			n			n			
ξ	−0.4	0	0.5	−0.4	0	0.5	−0.4	0	0.5	−0.4	0	0.5	$f''(\xi,0)$
0	0.0451	0.1404	0.2007	0.1021	0.2927	0.4059	0.2343	0.6459	0.8856	0.5736	1.5720	2.1522	0.3321
0.5	0.1602	0.2576	0.3234	0.2324	0.4338	0.5586	0.4041	0.8439	1.1082	0.8412	1.9146	2.5551	0.4797
1.0	0.4011	0.5136	0.5971	0.5195	0.7475	0.8971	0.7752	1.2679	1.5774	1.3918	2.5856	3.3285	0.8064
1.5	0.7925	0.8878	0.9718	0.8987	1.1690	1.3516	1.2564	1.8179	2.1799	2.0732	3.4029	4.2586	1.2387
2.0	1.3162	1.3890	1.4643	1.3571	1.6799	1.8955	1.8270	2.4664	2.8854	2.8583	4.3295	5.2890	1.7580
2.5	1.9398	1.9998	2.0667	1.8936	2.2680	2.5240	2.4802	3.2052	3.6852	3.7403	5.3587	6.4287	2.3579
3.0	2.6610	2.7132	2.7738	2.5400	2.9356	3.2307	3.2118	4.0289	4.5735	4.7133	6.4856	7.6681	3.0406
3.5	3.4801	3.5273	3.5831	3.3245	3.7077	4.0170	4.0214	4.9372	5.5499	5.7776	7.7113	9.0096	3.8166
4.0	4.3988	4.4424	4.4948	4.2399	4.5968	4.9062	4.9143	5.9143	6.6209	6.9426	9.0480	10.467	4.6973
4.5	5.4212	5.4624	5.5122	5.2726	5.6018	5.9097	5.8966	7.0314	7.7939	8.2173	10.506	12.054	5.6909
5.0	6.5550	6.5944	6.6423	6.4186	6.7249	7.0297	6.9732	8.2295	9.0748	9.6065	12.091	13.775	6.8044

and 100, with $\Omega_0 = 0$, 0.02, 0.1, 0.5, 1, 2, and ∞. To conserve space, these results are not listed here. Although calculations were carried out using the parameter Ω_0 to combine the curvature and buoyancy parameters in one independent variable ξ, results are more meaningful when presented in terms of the curvature parameter Λ and the mixed convection parameter χ. Two typical $Nu_x/(Re_x^{1/2}+Gr_x^{1/4})$ vs χ plots for the UWT case are shown in Figs. 5 and 6 for $Pr = 0.7$ and 7, respectively. In these figures the solid lines represent the actual runs for given values of Ω_0, while the dashed lines are found by interpolation of the computer output for the values of Λ presented. It can be seen from Figs. 5 and 6 that as the curvature

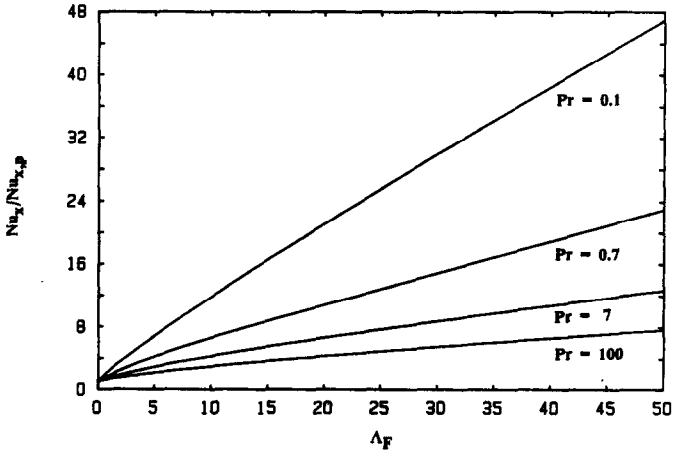

FIG. 3. $Nu_x/Nu_{x,p}$ vs Λ_F for pure forced convection, uniform wall temperature ($n = 0$).

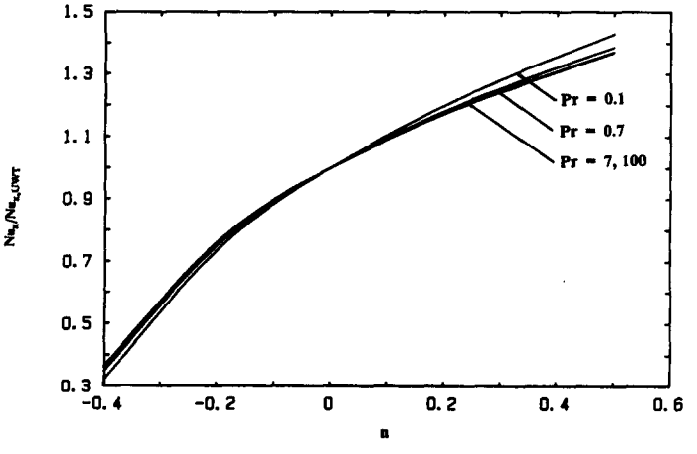

FIG. 4. $Nu_x/Nu_{x,UWT}$ vs n for pure forced convection, flat plates ($\Lambda_F = 0$).

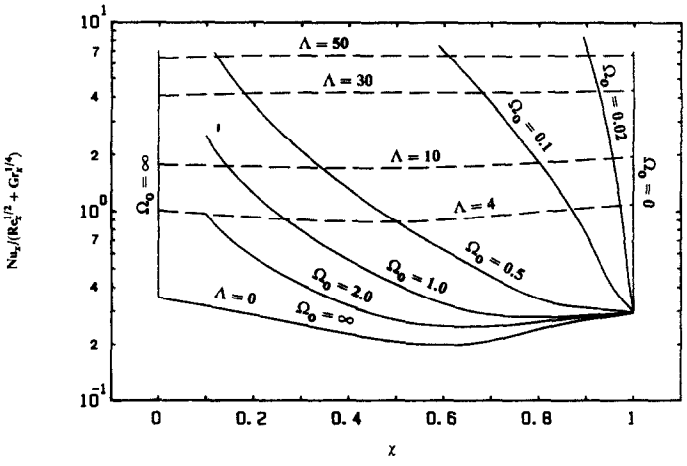

FIG. 5. $Nu_x/(Re_x^{1/2}+Gr_x^{1/4})$ vs χ for mixed convection, uniform wall temperature ($n = 0$), $Pr = 0.7$.

Λ increases for a constant value of χ the local Nusselt number increases. For small values of Ω_0, the effect of curvature is dominant in affecting the Nusselt number, whereas the buoyancy effect becomes dominant for larger values of Ω_0. When $\Omega_0 \to \infty$, either the flat plate solution is approached or the pure free convection case is approached. If the curves cut off at $\chi \leqslant 0.1$ were extended they would rise sharply to run between the curves for $\Omega_0 = 0.5$ and ∞, the pure free convection case. One can also observe from Figs. 5 and 6 that the curve for the flat plate ($\Lambda = 0$) is concave upward, and as χ decreases from 1 to 0 along the constant curvature curve of $\Lambda = 0$, the value of $Nu_x/(Re_x^{1/2}+Gr_x^{1/4})$ decreases to a minimum in the vicinity of $\chi = 0.6$ and then increases to its pure free convection value at $\chi = 0$. This can be seen more clearly in Fig. 7 for the flat plate, which also demonstrates that for $n \neq 0$ the curves run essentially parallel to the UWT curve.

The average Nusselt number results were also obtained, but they are not shown to conserve space. However, they are used to develop the correlation equation. It suffices to say that the trends of the curves are similar to those for the local Nusselt number.

For practical purposes, correlation equations were developed for the local and average Nusselt numbers. For pure free convection, for $0.1 \leqslant Pr \leqslant 100$, $-0.5 \leqslant n \leqslant 0.5$, and $0 \leqslant \Lambda \leqslant 50$ (with $\Lambda = \Lambda_N$), the correlation equation for the local Nusselt number is given by

$$Nu_x\, Gr_x^{-1/4} = \alpha_N(Pr)[A_N(\Lambda)+f_{1,N}(Pr)\Lambda](1+V_N W_N) \tag{30}$$

where

$$\alpha_N(Pr) = 0.75Pr^{1/2}[2.5(1+2Pr^{1/2}+2Pr)]^{-1/4} \tag{31}$$

$$A_N(\Lambda) = 1.4^{(1-0.7^{\Lambda})} \tag{32}$$

$$f_{1,N}(Pr) = 0.045+0.27Pr^{-0.46} \tag{33}$$

$$V_N = \{[0.88+0.5\exp(-2Pr^{1/4})]-0.77n\}n \tag{34}$$

$$W_N = \exp\{-[0.07+7.5\exp(-3.6Pr^{1/10})]\Lambda^{0.7}\}. \tag{35}$$

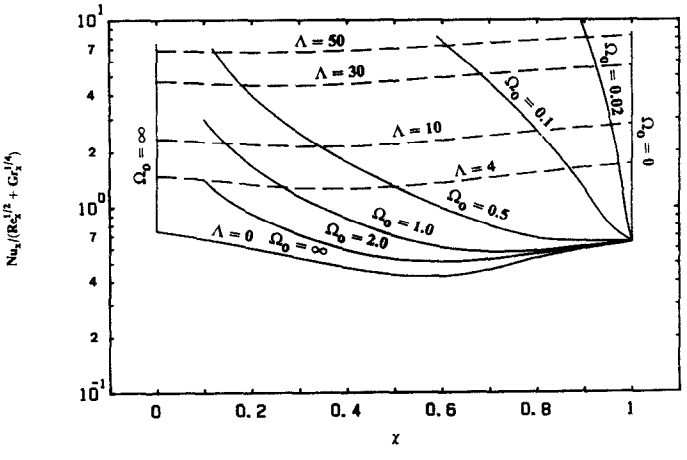

FIG. 6. $Nu_x/(Re_x^{1/2}+Gr_x^{1/4})$ vs χ for mixed convection, uniform wall temperature ($n = 0$), $Pr = 7$.

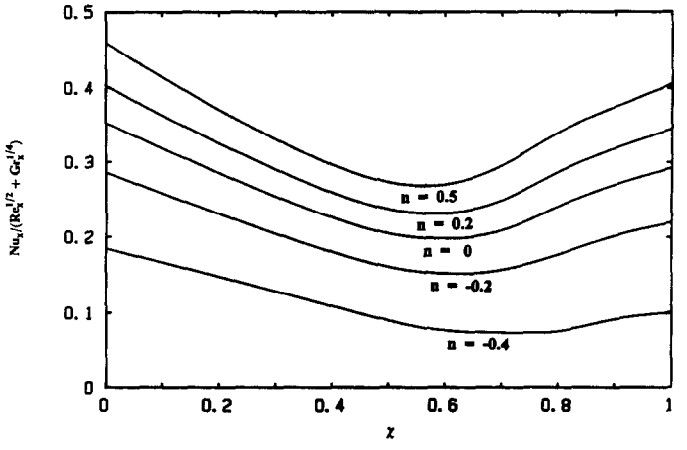

FIG. 7. $Nu_x/(Re_x^{1/2}+Gr_x^{1/4})$ vs χ for mixed convection, flat plates ($\Lambda = 0$), $Pr = 0.7$.

The average Nusselt numbers are correlated by

$$\overline{Nu}_L\, Gr_L^{-1/4} = \tfrac{4}{3}\alpha_N(Pr)[B_N(\Lambda)+f_{2,N}(Pr)\Lambda](1+\bar{V}_N) \tag{36}$$

where

$$B_N(\Lambda) = 1.4^{(1-0.75^{\Lambda})} \tag{37}$$

$$f_{2,N}(Pr) = 0.03+0.21Pr^{-0.44} \tag{38}$$

$$\bar{V}_N = (3V_N W_N - n\bar{W})/(3+n\bar{W}) \tag{39}$$

$$\bar{W} = \exp(-0.11\Lambda^{1.2}). \tag{40}$$

In equations (36)–(40), Λ now stands for Λ_N with $x = L$.

For the case of pure forced convection, for $0.1 \leqslant Pr \leqslant 100$, $-0.4 \leqslant n \leqslant 0.5$, and $0 \leqslant \Lambda \leqslant 50$ (with $\Lambda = \Lambda_F$), the correlation equation for the local Nusselt number is

$$Nu_x\, Re_x^{-1/2} = \alpha_F(Pr)[A_F(\Lambda)+f_{1,F}(Pr)\Lambda](1+V_F W_F) \tag{41}$$

where

$$\alpha_F(Pr) = 0.339Pr^{1/3}[1+(0.0468/Pr)^{2/3}]^{-1/4} \tag{42}$$

$$A_F(\Lambda) = (1+0.4\Lambda^{1/2}) \tag{43}$$

$$f_{1,F}(Pr) = 0.04+0.3Pr^{-0.45} \tag{44}$$

$$V_F = \{[1.17+11\exp(-5.6Pr^{1/10})]-0.92n\}n \tag{45}$$

$$W_F = \exp[-(0.07+0.3Pr^{-0.32})\Lambda^{3/5}]. \tag{46}$$

The correlation equation for the average Nusselt number is

$$\overline{Nu}_L\, Re_L^{-1/2} = 2\alpha_F(Pr)[B_F(\Lambda)+f_{2,F}(Pr)\Lambda](1+\bar{V}_F) \tag{47}$$

where

$$B_F(\Lambda) = (1+0.25\Lambda^{1/2}) \tag{48}$$

$$f_{2,F}(Pr) = (0.025+0.15Pr^{-0.45}) \tag{49}$$

$$\bar{V}_F = V_F \exp[-(0.06+0.17Pr^{-1/3})\Lambda^{0.65}]. \tag{50}$$

In equations (47)–(50), Λ stands for Λ_F with $x = L$.

It should be noted that the form of these correlation equations is such that for the UWT case V_N, V_F, $\bar{V}_N$, $\bar{V}_F$ are zero and they drop out from equations (30), (36), (41), and (47). Also, the forms of A_N, A_F, B_N, and B_F are such that for $\Lambda = 0$ they become one, and for the flat plate UWT case only α_N and α_F are needed. The expression for α_N is taken from Ede [26] and the expression for α_F is taken from Churchill and Ozoe [27]. The error in equations (30) and (36) is less than 8.5% for the UWT case and less than 13.5% for $-0.5 \leqslant n \leqslant 0.5$. The maximum error in equations (41) and (47) is about 9.2% for the UWT case and about 14.5% for $-0.4 \leqslant n \leqslant 0.5$.

Following Churchill [22], the correlation equation for Nusselt numbers in mixed convection is expressed as

$$\left(\frac{Nu}{Nu_F}\right)^m = 1+\left(\frac{Nu_N}{Nu_F}\right)^m$$

$$\left(\frac{Nu}{Nu_N}\right)^m = 1+\left(\frac{Nu_F}{Nu_N}\right)^m. \tag{51}$$

This form of correlation has been found to give an accuracy of about 5% for $0.1 \leqslant Pr \leqslant 100$ for flat plates with $m = 3$ and was also verified experimentally for air in the UWT case [16, 17]. For the present study with a single mixed convection parameter χ, the corresponding correlation equation can be represented by

$$\frac{Nu_x}{(Re_x^{1/2}+Gr_x^{1/4})} = \left\{\left[\chi\left(\frac{Nu_x}{Re_x^{1/2}}\right)_F\right]^m + \left[(1-\chi)\left(\frac{Nu_x}{Gr_x^{1/4}}\right)_N\right]^m\right\}^{1/m}. \tag{52}$$

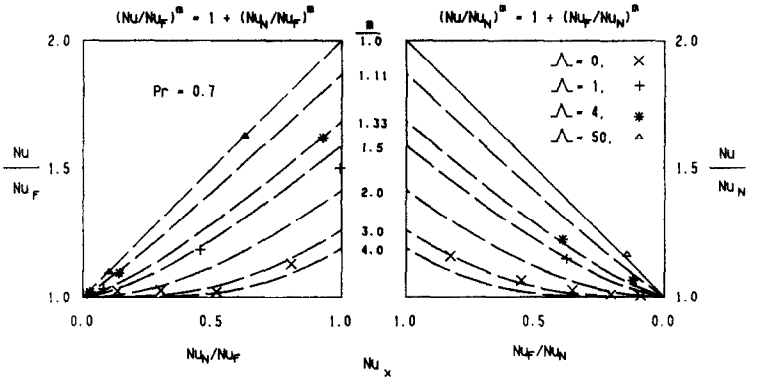

FIG. 8. Development of the local Nusselt number correlation equation for buoyancy-assisting, mixed convection.

This equation is generally valid for vertical cylinders with a power law variation in the surface temperature, in which the exponent m depends on the Prandtl number and the surface curvature parameter. The graphical technique of Churchill [22] was used to determine the relationship among m, Λ, and Pr for the UWT case. Figure 8 shows a sample graph for $Pr = 0.7$. In this graph Nu_F is the Nusselt number as a function of $\Lambda_F = \Lambda$, Pr, and n for the pure forced convection case and Nu_N is the Nusselt number as a function of $\Lambda_N = \Lambda$, Pr, and n for the pure free convection case. That is, they are calculated from the endpoints of the curves in the Nusselt number figures at $\chi = 1$ and 0 for lines of constant Λ for given Pr and n. Reference lines for various values of m are plotted and points corresponding to various curvatures are marked with different symbols in the figure. For $Pr = 0.7$ it is seen from Fig. 8 that as the curvature increases from $\Lambda = 0$ to 50 the value of m decreases from about 3 to about 1. The resulting expression for $m(Pr, \Lambda)$ for the UWT case is determined as

$$m = 1 + 2\exp[-(0.8 + 0.55Pr^{-0.34})\Lambda^{0.3}]. \quad (53)$$

It was found that equation (52) is applicable to flat plates ($\Lambda = 0$) for $-0.4 \leqslant n \leqslant 0.5$ with $m = 3$. For cylinders ($\Lambda > 0$), equation (52) along with equation (53) can be used for $n > 0$ but it gives inconsistent results for $n < 0$. For the ranges of Pr, Λ, and $n \geqslant 0$ studied, equation (52) along with the m expression from equation (53) produce results that are valid to within about 9% when using computer output for Nu_F and Nu_N and to within about 14% when using equations (30) and (41). Equation (52) was also found to be valid for the average Nusselt number with the same accuracy for $n \geqslant 0$ if Nu_x, Re_x, Gr_x, and χ in the equation are replaced, respectively, by $\overline{Nu}_L$, Re_L, Gr_L, and χ_L. A reliable relationship for $n < 0$ was not obtained, but equations (52) and (53) should provide satisfactory results for both the local and average Nusselt numbers.

As a final note, it must be pointed out that the Nusselt number results and the corresponding correlation equations presented in this study are for laminar, axisymmetric boundary layer flows along slender vertical cylinders, without flow separation at the leading edge of the cylinder. The validity of the present numerical results for mixed convection can only be verified with experimental data which are currently lacking. Thus, in applying these results, care should be exercised, and the Reynolds and Grashof numbers should be limited to values within the laminar regime (i.e. for $Re_x \leqslant 10^5$ and $Gr_x \leqslant 10^9$).

CONCLUSIONS

Mixed convection along a vertical cylinder with an arbitrary variation in the surface temperature is analyzed for the entire regime ranging from pure free convection to pure forced convection. Numerical results are presented for the case of $T_w(x) - T_\infty = ax^n$. It is found that the local Nusselt number $Nu_x/(Re_x^{1/2} + Gr_x^{1/4})$ increases with increasing Prandtl number, increasing value of the exponent n, and increasing curvature for the entire mixed convection regime ranging from pure free convection ($\chi = 0$) to pure forced convection ($\chi = 1$). For the vertical flat plate, this quantity initially decreases as χ is decreased from 1 and then increases to the pure free convection value as χ approaches 0. However, as the curvature Λ increases the $Nu_x/(Re_x^{1/2} + Gr_x^{1/4})$ vs χ curve for a constant curvature tends to become linear and lie on a line with end points at $\chi = 0$ and 1. The average Nusselt number $\overline{Nu}_L/(Re_L^{1/2} + Gr_L^{1/4})$ follows a similar pattern as that for the local Nusselt number. The effects of both the Prandtl number and n on the Nusselt numbers diminish as the curvature increases, but remain significant for curvatures $\Lambda \leqslant 50$ when Prandtl numbers are large. Correlation equations for the local and average Nusselt numbers are also given.

REFERENCES

1. T. S. Chen and A. Mucoglu, Buoyancy effects on forced convection along a vertical cylinder, *J. Heat Transfer* **97**, 198–203 (1975).

2. A. Mucoglu and T. S. Chen, Buoyancy effects on forced convection along a vertical cylinder with uniform surface heat flux, *J. Heat Transfer* **98,** 523–525 (1976).
3. M. N. Bui and T. Cebeci, Combined free and forced convection on vertical cylinders, *J. Heat Transfer* **107,** 476–478 (1985).
4. S. L. Lee, T. S. Chen and B. F. Armaly, Mixed convection along isothermal vertical cylinders and needles, *Proc. Eighth Int. Heat Transfer Conf.*, Vol. 3, pp. 1425–1432 (1986).
5. S. L. Lee, T. S. Chen and B. F. Armaly, Mixed convection along vertical cylinders and needles with uniform surface heat flux, *J. Heat Transfer* **109,** 711–716 (1987).
6. S. L. Lee, T. S. Chen and B. F. Armaly, New finite difference solution methods for wave instability problems, *Numer. Heat Transfer* **10,** 1–8 (1986).
7. R. L. Burden and J. D. Faires, *Numerical Analysis* (3rd Edn), pp. 117–129. Prindle, Weber and Schmidt, Boston (1985).
8. W. Elenbaas, The dissipation of heat by free convection from vertical and horizontal cylinders, *J. Appl. Phys.* **19,** 1148–1154 (1948).
9. E. M. Sparrow and J. L. Gregg, Laminar-free-convection heat transfer from the outer surface of a vertical circular cylinder, *Trans. ASME* **78,** 1823–1829 (1956).
10. H. K. Kuiken, Axisymmetric free convection boundary layer flow past slender bodies, *Int. J. Heat Mass Transfer* **11,** 1141–1153 (1968).
11. T. Fujii and H. Uehara, Laminar natural convective heat transfer from the outer surface of a vertical cylinder, *Int. J. Heat Mass Transfer* **13,** 607–615 (1970).
12. W. J. Minkowycz and E. M. Sparrow, Local nonsimilar solutions for natural convection on a vertical cylinder, *J. Heat Transfer* **96,** 178–183 (1974).
13. H. K. Kuiken, The thick free-convection boundary layer along a semi-infinite isothermal vertical cylinder, *J. Appl. Math. Phys. (ZAMP)* **25,** 497–514 (1974).
14. H. R. Lee, T. S. Chen and B. F. Armaly, Natural convection along vertical cylinders with variable surface temperature, *J. Heat Transfer* **110,** 103–108 (1988).
15. J. J. Heckel, T. S. Chen and B. F. Armaly, Natural convection along slender vertical cylinders with variable surface heat flux, *J. Heat Transfer* (1989), in press.
16. T. S. Chen, B. F. Armaly and N. Ramachandran, Correlations for laminar mixed convection flows on vertical, inclined, and horizontal flat plates, *J. Heat Transfer* **108,** 835–840 (1986).
17. N. Ramachandran, B. F. Armaly and T. S. Chen, Measurements and predictions of laminar mixed convection flow adjacent to a vertical surface, *J. Heat Transfer* **107,** 636–641 (1985).
18. A. Mucoglu and T. S. Chen, Mixed convection on inclined surfaces, *J. Heat Transfer* **101,** 422–426 (1979).
19. J. Gryzagoridis, Combined free and forced convection from an isothermal vertical plate, *Int. J. Heat Mass Transfer* **18,** 911–916 (1975).
20. M. S. Raju, X. Q. Lin and C. K. Law, A formulation of combined forced and free convection past horizontal and vertical surfaces, *Int. J. Heat Mass Transfer* **17,** 2215–2224 (1984).
21. J. R. Lloyd and E. M. Sparrow, Combined forced and free convection flow on vertical surfaces, *Int. J. Heat Mass Transfer* **13,** 434–438 (1970).
22. S. W. Churchill, A comprehensive correlating equation for laminar assisting, forced and free convection, *A.I.Ch.E. Jl* **23,** 10–16 (1977).
23. B. Gebhart, *Heat Transfer* (2nd Edn), p. 340. McGraw-Hill, New York (1971).
24. T. S. Chen, H. C. Tien and B. F. Armaly, Natural convection on horizontal, inclined, and vertical plates with variable surface temperature or heat flux, *Int. J. Heat Mass Transfer* **29,** 1465–1478 (1986).
25. R. A. Seban and R. Bond, Skin friction and heat-transfer characteristics of a laminar boundary layer on a cylinder in axial incompressible flow, *J. Aeronaut. Sci.* **18,** 671–675 (1951).
26. A. J. Ede, Advances in free convection, *Adv. Heat Transfer* **4,** 1–64 (1967).
27. S. W. Churchill and H. Ozoe, Correlations for laminar forced convection in flow over an isothermal flat plate and in developing and fully developed flow in an isothermal tube, *J. Heat Transfer* **95,** 416–419 (1973).

CONVECTION MIXTE SUR DES CYLINDRES VERTICAUX MINCES AVEC UNE TEMPERATURE VARIABLE SUR LA SURFACE

Résumé—La convection mixte à couche limite laminaire le long de cylindres verticaux minces est analysée pour une température de la surface $T_w(x)$ qui varie arbitraitement en fonction de la coordonnée axiale x. Elle couvre le régime complet de convection mixte depuis la convection naturelle pure ($\chi = 0$) jusqu'à la convection forcée pure ($\chi = 1$) où $\chi = [1+(Gr_x/Re_x^2)^{1/4}]^{-1}$. Les équations de couche limite et les conditions aux limites sont d'abord mises sous forme adimensionnelle par une transformation sans similitude et le système d'équations résultant est ensuite résolu par une méthode pondérée de différences finies en conjonction avec une interpolation spline cubique. Das calculs sont effectués dans le cas d'une variation en puissance pour la température de surface $T_w(x)-T_\infty = ax^n$, pour des fluides avec des nombres de Prandtl de 0,1, 0,7, 7 et 100, dans un domaine large des paramètres de courbure de la surface $0 \leqslant \Lambda \leqslant 50$ (ou $0 \leqslant \xi \leqslant 5$). On présente les nombres de Nusselt locaux et moyens. On trouve que le nombre de Nusselt local dans la forme $Nu_x/(Re_x^{1/2}+Gr_x^{1/4})$ augmente avec la courbure de la surface, le nombre de Prandtl et l'exposant n, mais pour des valeurs faibles de Λ, il décroît d'abord puis il croît lorsque χ varie de 0 à 1. Quand la courbure augmente, on trouve une relation linéaire entre le nombre de Nusselt et le paramètre de convection mixte. Des formules sont présentées pour les nombres de Nusselt locaux et moyens.

MISCHKONVEKTION AN EINEM SCHLANKEN SENKRECHTEN ZYLINDER MIT VERÄNDERLICHER OBERFLÄCHENTEMPERATUR

Zusammenfassung—Für den Fall, daß sich die Oberflächentemperatur $T_w(x)$ an einem senkrechten Zylinder willkürlich mit der Länge ändert, wird die Mischkonvektion in der laminaren Grenzschicht analysiert. Als charakteristische Größe wird dabei der Parameter $\chi = [1 + (Gr_x/Re_x^2)^{1/4}]^{-1}$ verwendet und der gesamte Bereich der Mischkonvektion von der freien Konvektion ($\chi = 0$) bis zur erzwungenen Konvektion ($\chi = 1$) untersucht. Die maßgebende Grenzschichtgleichung und die Randbedingungen an der Grenzschicht werden durch eine nichtlineare Umformung zuerst in eine dimensionslose Form gebracht und anschließend das entstehende Gleichungssystem mit Hilfe einer gewichteten Finite-Elemente-Methode in Kombination mit einer kubischen Spline-Interpolation gelöst. Berechnungen werden beispielhaft für eine, sich nach dem Potenzansatz $T_w(x) - T_\infty = ax^n$ ändernde Oberflächentemperatur für Fluide mit Prandtl-Zahlen von 0,1; 0,7; 7 und 100 und in einem weiten Bereich des Parameters der Oberflächenkrümmung ($0 \leqslant \Lambda \leqslant 50$ bzw. $0 \leqslant \xi \leqslant 5$) durchgeführt. Örtliche und mittlere Nusselt-Zahlen werden vorgestellt. Es zeigt sich, daß die lokale Nusselt-Zahl der Form $Nu_x/(Re_x^{1/2} + Gr_x^{1/4})$ mit steigender Oberflächenkrümmung, Prandtl-Zahl und dem Exponent n zunimmt. Wird χ von 0 auf 1 gesteigert, so nimmt die Nusselt-Zahl zunächst ab und wird dann wieder größer. Bei wachsender Krümmung ergibt sich ein linearer Zusammenhang zwischen der Nusselt-Zahl und dem Parameter (χ) der Mischkonvektion. Abschließend werden Korrelationsgleichungen für örtliche und gemittelte Nusselt-Zahlen angegeben.

СМЕШАННАЯ КОНВЕКЦИЯ ВДОЛЬ ВЕРТИКАЛЬНЫХ ЦИЛИНДРОВ МАЛОГО ДИАМЕТРА С ИЗМЕНЯЮЩЕЙСЯ ТЕМПЕРАТУРОЙ ПОВЕРХНОСТИ

Аннотация—Анализируется смешанная ламинарная конвекция в пограничном слое вдоль вертикальных цилиндров малого диаметра при произвольном изменении температуры поверхности $T_w(x)$ по осевой координате x. Исследуются все режимы смешанной конвекции от чисто свободной ($\chi = 0$) до чисто вынужденной ($\chi = 1$), где $\chi = [1 + (Gr_x/Re_x^2)^{1/4}]^{-1}$ является параметром смешанной конвекции. Определяющие уравнения пограничного слоя и граничные условия приводятся сначала к безразмерному неавтомодельному виду, а затем полученная система уравнений решается при помощи взвешенного конечно-разностного метода в сочетании с кубической сплайн-интерполяцией. Проведены расчеты смешанной конвекции для случая степенного изменения температуры поверхности $T_w(x) - T_\infty = ax^n$ для жидкостей с числами Прандтля 0,1; 0,7; 7 и 100 в широком диапазоне изменения параметров кривизны поверхности $0 \leqslant \Lambda \leqslant 50$ (или $0 \leqslant \xi \leqslant 5$). Представлены локальные и средние значения числа Нуссельта. Найдено, что локальное число Нуссельта, представленное в виде $Nu_x/(Re_x^{1/2} + Gr_x^{1/4})$, увеличивается с возрастанием кривизны поверхности, числа Прандтля и показателя степени n, при низких же значениях Λ оно сначала уменьшается, а затем увеличивается с изменением χ от 0 до 1. Найдено, что по мере увеличения кривизны между числом Нуссельта и параметром смешанной конвекции χ устанавливается линейная зависимость. Также представлены корреляционные уравнения для локального и среднего чисел Нуссельта.